Chemically induced solidification – a new way to produce thin solid-near- net shapes

Carl Slater, Stephen Spooner, Claire Davis and Seetharaman Sridhar

Email: c.d.slater@warwick.ac.uk, Tel:+4424 76151577

WMG, University of Warwick, Coventry, UK

Abstract

In-situ observation of the solidification of high carbon steel (4 wt% C) through decarburization has been carried out as a feasibility study into reducing high power usage and high CO_2 production involved in steel making. Decarburization has been carried out under both air and pure N_2 atmospheres at temperature of 1573K (1300 °C) and 1673K (1400 °C). A solidified shell of around 500µm was formed with carbon concentrations reduced down to 1% in as short as 18s.

Keywords

Liquid Steel; Decarburization; Solidification; Belt Casting; In-situ Observation

Introduction

In 2012 Park *et al.* [1] suggested the feasibility of decarburising of 4wt% C cast iron in solid state during the continuous strip casting process using oxidising gases (such as CO_2 and H_2O), entitled the S^3 process. The advantage of such a process would be that aspects of the steelmaking process, such as the basic oxygen furnace (BOF) can be circumvented. Therefore avoiding large amounts of oxygen and unwanted oxide inclusion products. Although the results showed promise, decarburization rates to 0.5 wt% were in excess of 30mins for a 1 mm strip. Later the S^3-II [2] process was proposed where some decarburization occurs in the tundish (down to 1.2-1.9wt%) by bubbling O_2 before further solid state decarburization. Decarburising to this point in the liquid ensures no excess oxygen to form oxides, and thus still achieves "clean" steel production. This reduced solid state decarburization times to around 10mins for 1 mm strips held at 1473K (1200 °C).

Belt casting (particularly horizontal single belt casting (HSBC)) offers the unique possibility to introduce gases during the solidification of steel and affect the steel chemistry through the strip thickness thanks to the thin cross section. This opens up the possibility to expand on the premise of the S^3-II process and decarburise to a lower carbon fraction in the liquid to the point of solidification (a limit not desirable to attain in the tundish). Therefore, the aim of this work is to understand and observe the isothermal solidification of liquid iron similar in composition to pig iron by means of decarburization in both air and N_2 atmospheres. This therefore explores the feasibility of an inline continuous decarbusrising and non-CO_2 forming (in the case of N_2) method of producing steel whilst also allowing for a different solidification structure. The limit of decarburization in this case may be the balance between the desirable removal of carbon and un-desirable dissolution of interstitials (oxygen and nitrogen) and the formation of oxides (and other such undesirably products of interaction with these gases).

Materials and Methods

A high temperature confocal scanning laser microscope (CSLM) was used to observe the in-situ solidification of the molten steel (an outline of the CSLM technique has been covered in a previous paper [3]). A Fe-4C-0.2P steel was used for this study and samples were machined to cubes of around 0.25g. The purpose of phosphorous addition was to enable the solidification structure to be revealed. The samples were heated at 10 K/s to a set peak temperature under argon (with and O_2 concentration < 2ppm and a flow rate of 200 ml/min), and after a 15s hold the atmosphere was switched to a decarburising atmosphere (either air or N_2) at a slow rate of 100 ml/min. As decarburization occurs the sample travels along the depicted line in Figure 1 until solidification of the observable surface appeared to be completed, after which the atmosphere was switched immediately back to Ar before cooling to room temperature (at a rate of 1 K/s). The time taken for replacing the gas atmosphere in the chamber twice is estimated to be 30s and is described in the previous works [3].

Results and Discussion

Figure 1 shows an example time lapse of the solidification of the pig iron under an air atmosphere at 1573K (1300 °C). It can be seen that three distinct phases are present; liquid, austenite (as indicated by the first solid phase appearing in the pathways shown in Figure 1) and a particulate (which appears almost instantly once the atmosphere changes). The particulate phase has been proven to be carbon enriched through SEM-EDS mapping (an intensity of over 10 times that seen in the bulk material) of several particle examples found on the surface of a test sample quenched in a nitrogen atmosphere as soon as the particulate phase formed. The sample was taken straight to SEM to avoid contamination, and multiple scans of the same area conducted to remove the possibility of carbon deposition during analysis being the cause of detection; the phase showed a depletion in oxygen compared to the main matrix, removing the possibility of this being oxide formation. Figure 2 shows the phase distribution of the system with varying N content, it is clearly seen that as mass percent of N in the liquid steel increases beyond 1 wt% the formation of graphite occurs under equilibrium conditions. This is possible if we consider the interaction between nitrogen and the surface of the steel as its own system (as it is this interface where the graphite is shown to form) [3].

A summary of the critical points of the solidification process can be seen in Table 1 for all the conditions assessed. For the conditions in air a clear increase in the time to first solid was seen with increasing temperature, however the time from first solid to last liquid (transformation time) decreased with temperature. These trends are consistent with the phase diagram where at higher temperatures more carbon needs to be removed to start solidification, however the mushy zone width is much narrower than at lower temperatures.

Decarburization with oxygen in the air forms a mixture of CO and CO_2, these molecules will form a boundary layer at the surface of the metal if the production of CO/CO_2 is greater than the diffusion of the gases away from the surface [4]. Previous reports by Sain [5] and Fruehan [6] indicate that the interfacial reaction between oxygen and carbon is very fast and gas molecule sticking parameters are very low (step 5) at these temperatures. Mass transfer in the bulk phases have been reported to be slower and therefore are likely to be rate controlling. Of these mass transports it is O_2 diffusion through the boundary layer that is likely the dominant rate controlling factor due to the low driving

force of oxygen through this layer. This is supported in levitated droplet experiments [7][8] where swelling is observed and discussion of limited diffusion of the reactant gases away from the interface is the given reasoning.

In the case of nitrogen the reaction produces a combination of C_2N_2 (cyanogen) and XCN (variable cyanides) and the reaction steps are similar to that of decarburization with air, however following the reported rates of nitrogen absorption into the melt [9] the rate of decarburization required for the viewed solidification in nitrogen would not be possible. As such it is suggested that decarburization with nitrogen is dominated through the pathway of either atomic or diatomic nitrogen reaction with precipitated the carbon enriched particulate phase. Decarburization by nitrogen reaction with graphite is further supported by the observed retardation of the reaction at higher temperatures. Previous findings [10] report the reduced reaction rate of graphite and nitrogen at higher temperatures due to the rate of graphite "healing" being increased more than the rate of gasification with temperature (where the balance between reactant and products moves to reduce the rate of decarburization). In the case of nitrogen, no noticeable surface contamination (such as the oxide layer seen in air) was observed, suggesting that post solidification decarburization can continue under this atmosphere (although the rate limiting steps may change).

Figure 3a shows the as cast microstructure of the high carbon iron used in this study that has been melted and re-solidified in argon. A solidified dendritic structure can be seen, these dendrites form as austenite and on further cooling transform to pearlite. Whilst the interdendritic regions are enriched in carbon, subsequently graphite can be seen in a ferrite matrix. The samples where decarburization has occurred showed a decarburised shell (consistently around 300-500 µm thick, Figure 3b) and micrographs of this shell can be seen in Figure 4c-e. Here pro-eutectoid cementite can be seen in a pearlite matrix. Based on the level of cementite (area percent values of 11.7, 3.3, 15.4 for Figure 4c-e respectively) then the amount of carbon in this region can be calculated by the lever rule to be 1.48, 0.99 and 1.7 wt% respectively.

Conclusions

The results shown here suggest that the feasibility of decarburization of high carbon steel can be achieved down to lower carbon levels than the S^3 process and in a shorter period of time whilst the steel is liquid. Particularly under a N2 atmosphere, samples with around a 0.5 mm decarburised layer (between 1-1.7 wt% carbon remaining) were produced with very little/no observable contamination on the surface. This suggests that this is a "clean" method of decarburising steel that can be implemented inline of the continuous casting process, whilst also having the potential of bypassing certain steel making processes such as the BOF. The results also suggest that a layered microstructure can be achieved and layer thicknesses potentially controlled by the duration of gas exposure conditions (flow rate and gas chemistry).

Acknowledgements

The authors would like to thank EPSRC for funding (grant number EP/M014002/1) and also WMG for their support and facilities.

References

1. J. Park, T. Van Long, and Y. Sasaki, Tetsu-to-Hagané **98**, 26 (2012).

2. W.-H. Lee, J.-O. Park, J.-S. Lee, J. A. de Castro, and Y. Sasaki, Ironmak. Steelmak. **39**, 530 (2012).

3. C. Slater, S. Spooner, C. Davis, and S. Sridhar, Mater. Lett. **173**, 98 (2016).

4. H. Schliching, *Boundry-Layer Theory*, 7th ed. (McGraw-Hill, New York, 1979).

5. D. R. Sain and G. R. Belton, Metall. Mater. Trans. B **7B**, 235 (1976).

6. R. J. Fruehan and L. J. Martonik, Metall. Mater. Trans. B **5**, 1027 (1974).

7. E. Chen and K. S. Coley, Ironmak. Steelmak. **37**, 541 (2010).

8. C. Molloseau and R. Fruehan, Metall. Mater. Trans. B (2002).

9. R. J. Fruehan and L. J. Martonik, Metall. Trans. B **11**, 615 (1980).

10. C. F. Cullis and J. G. Yates, Trans. Faraday Soc. **60**, 141 (1964).

Table

Table 1: Summary of the time taken for first solid and last liquid to occur under different amtopheric conditions.

Temperature (K)	Atmosphere*	Time to first solid (s)	Time to last liquid (s)	Transformation time (s)
1573	Argon	Not observed	Not observed	-
1673	Argon	Not observed	Not observed	-
1773	Argon	Not observed	Not observed	-
1573	Air	7	18	11
1673	Air	11	18	7
1773	Air	34	39	4
1573	N2	32	155	123
1673	N2	Not observed	Not observed	-
1673	N2 (increased rate of 400ml/min)	265	841	576

*All tests were carried out with an atmospheric flow rate of 100 ml/min unless otherwise stated.

List of Figures

Figure 1: The Fe-C phase diagram showing the path of solidification through decarburization (blue) and time lapse image showing the solidification through decarburization (from right to left) in air at 1300 °C (with times related to the point of gas switch over).

Figure 2: Thermocalc prediction showing the stabilisation of graphite in the presence of N.

Figure 3: Micrgraphs of samples etched in 3% Nital a) pig iron cast in argon, b) an unetched sample showed the solidified shell, c) decarburised at 1573K (1300 °C) in air, d) decarburised at 1573K (1300 °C) in N and e) decarburised at 1673K (1400 °C) in N.

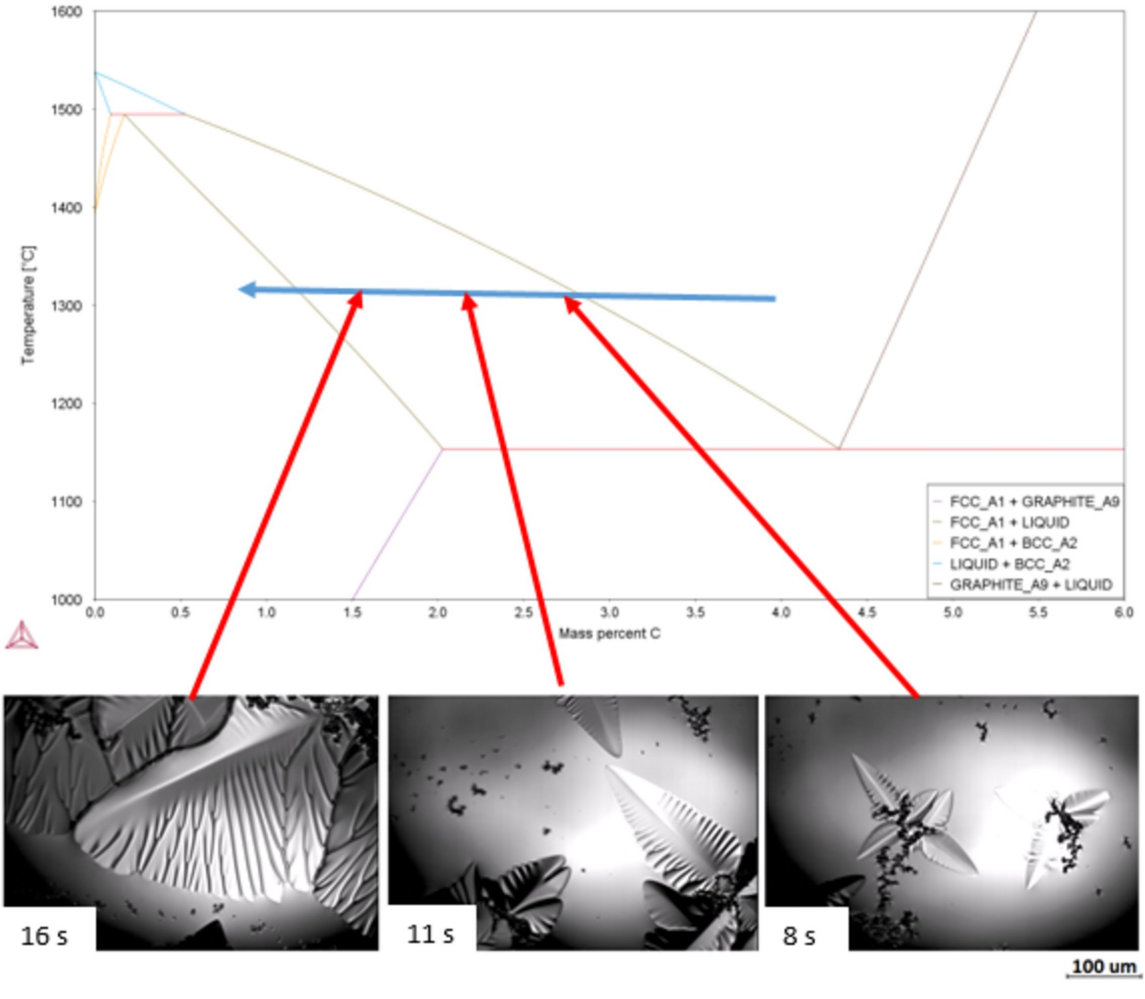
1600
1500
1400
1300
1200
1100
1000
Temperature [°C]
0.0
0.5
1.0
1.5
2.0
2.5
3.0
3.5
4.0
4.5
5.0
5.5
6.0
Mass percent C
FCC_A1 + GRAPHITE_A9
FCC_A1 + LIQUID
FCC_A1 + BCC_A2
LIQUID + BCC_A2
GRAPHITE_A9 + LIQUID
16 s
11 s
8 s
100 um

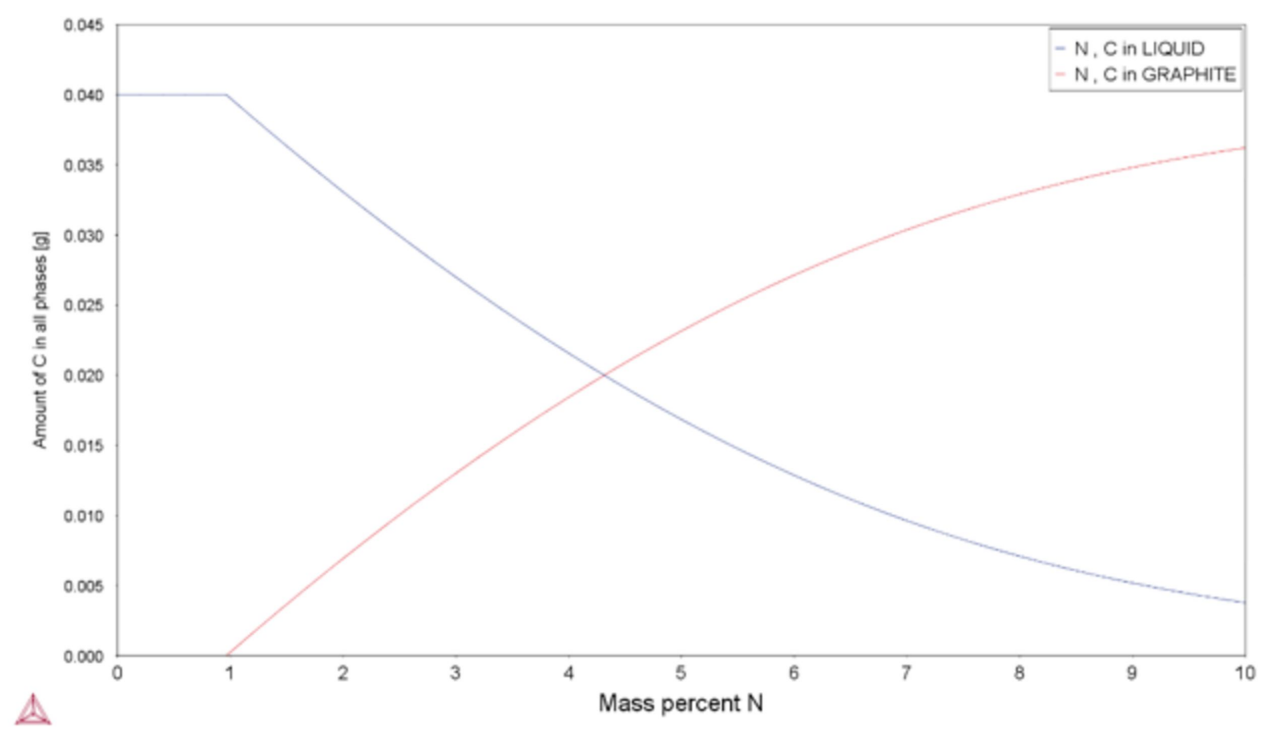
N , C in LIQUID
N , C in GRAPHITE
Amount of C in all phases [g]
0.045
0.040
0.035
0.030
0.025
0.020
0.015
0.010
0.005
0.000
0
1
2
3
4
5
6
7
8
9
10
Mass percent N

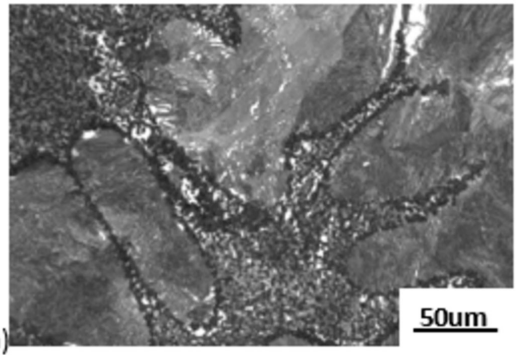

a)

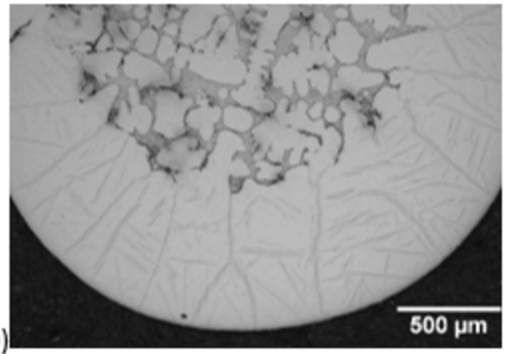

b)

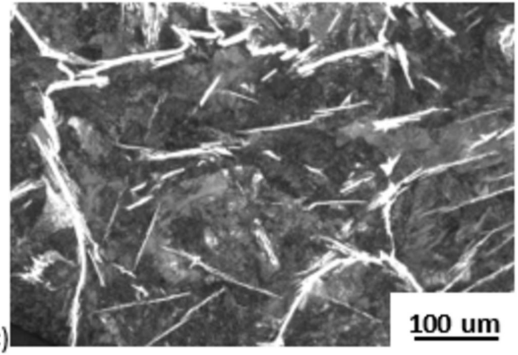

c)

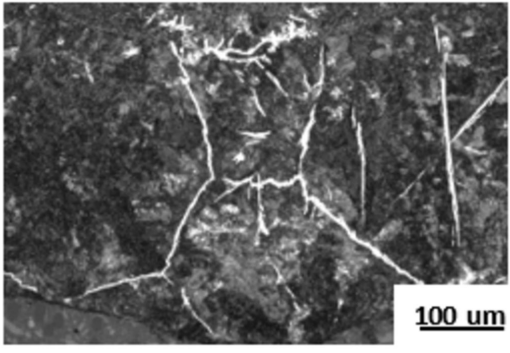

d)

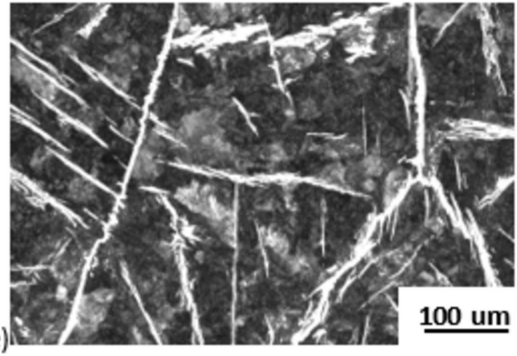

e)